A matrix isolation study of the C_s symmetric OCNO(X ^{2}A″) radical

Corey S. Jamieson,[a] Alexander M. Mebel[b] and Ralf I. Kaiser*[ac]

[a] Department of Chemistry, University of Hawaii at Manoa, Honolulu, HI 96822, USA
[b] Department of Chemistry and Biochemistry, Florida International University, Miami FL, 33199, USA
[c] Department of Physics and Astronomy, The Open University, Milton Keynes, UK MK7 6AA. E-mail: kaiser@gold.chem.hawaii.edu

Here we report the first experimental detection of the C_s symmetric nitroformyl radical, OCNO(X ^{2}A″) in a nitrogen–carbon dioxide matrix at 10 K using a Fourier transform infrared spectrometer (FTIR). The ν_1 vibrational frequency was observed at 2113 cm^{-1}. This assignment was confirmed by follow-up experiments using isotopically labeled reactant molecules (^{15}N, ^{18}O, ^{13}C). To synthesize this radical, we irradiated solid nitrogen–carbon dioxide ice mixtures with energetic electrons at 10 K. Suprathermal nitrogen atoms in their electronic ground and/or first electronically excited state were generated via the radiation induced degradation of molecular nitrogen; these atoms could then react with carbon dioxide to eventually yield the nitroformyl radical. We also investigated the kinetics of the formation of the nitroformyl radical and support the arguments with computations on the doublet and quartet OCNO potential energy surfaces (PESs).

1. Introduction

The bent OCNO radical (C_s, X ^{2}A″) presents an important intermediate in combustion flames as well as atmospheric and astronomical environments.[1–3] However, a literature search yields only sparse accounts of this molecule. Electronic structure calculations suggest that two resonance structures of this molecule exist (Fig. 1); the first where the unpaired electron resides on the oxygen atom at the nitrogen terminus (structure A) and the second where the unpaired electron resides on the carbon atom (structure B). In their calculations, Benson and Francisco[1] found the optimized structure to lie between the two resonance forms. The NCO bond angle of the lowest energy structure was calculated to be around 155° compared to the NCO bond angles of the resonance structures of 180 and 108°, respectively. This means that the central C–N bond has both single and double bond character, a result also supported with bond length calculations by Benson and Francisco (1.283 Å).

Even though the aforementioned paper has well characterized the energy, structure, and vibrational frequencies of the nitroformyl radical (OCNO), it has proven to be a difficult molecule to experimentally confirm. This is due to a relatively low-energy dissociation pathway that leads to a carbon monoxide molecule (CO, X $^1\Sigma^+$) and nitric oxide (NO, X $^2\Pi$) as seen in eqn (1). Korkin et al.[4] calculated the energy barrier for dissociation to be 10.5 kJ mol^{-1} with respect to the reactant and a total reaction exoergicity of 133.9 kJ mol^{-1} along the ^{2}A″ surface. More recently, Cooksy has investigated the mechanism of the lowest energy dissociation pathway in addition to the overall thermodynamics.[5] He found that rather than following the ^{2}A″ surface to dissociate, the molecule may alter its symmetry to more closely resemble resonance structure B from Fig. 1. This occurs by out-of-plane bending of the OCN angle causing tension on the C–N bond. Cooksy suggested that this deformation process has a barrier of 15 kJ mol^{-1} to reach

the geometry of resonance structure B which may be more conducive to dissociation.

$$OCNO(X\ ^2A'') \rightarrow CO(X\ ^1\Sigma^+) + NO(X\ ^2\Pi) \qquad (1)$$
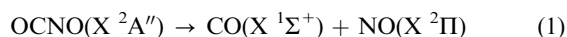
To our knowledge, there still has been neither an investigation of the formation pathways to the nitroformyl radical nor experimental evidence of its existence. In this work we present the first experimental detection of the nitroformyl radical via the reaction of suprathermal nitrogen atoms with carbon dioxide and understand its formation pathways by analyzing the kinetics of the reaction, the mechanism of formation, and the energetics associated with the potential energy surface (PES). This study also has relevance to the chemistry that occurs in the cold environment of interstellar space where the temperature (10 K) is more favorable for isolating unstable reaction intermediates such as the nitroformyl radical (OCNO). We will also compare the dynamics of the N/CO$_2$ system with the recently investigated O/CO$_2$ system.[6]

2. Experimental

The experiments were carried out in a contamination free ultra high vacuum stainless steel chamber.[6] The chamber can reach pressures down to 5×10^{-11} Torr by use of a magnetically suspended turbo molecular pump (TMP) that is backed by a scroll pump. All pumps used are oil-free to ensure no hydrocarbon contaminants enter the system. Temperatures of 10 K are reached using a two-stage closed-cycle helium refrigerator that is interfaced directly to a polished single crystal silver mirror onto which the ices are condensed. The silver substrate is suspended by a differentially pumped rotatable feedthrough, which aligns the wafer in the center of the main chamber. Gas condensation is carried out at 10 K where the pressure is regulated by a thermovalve that lets gas through the linear transfer mechanism and to the gas capillary array which evenly disperses the gas. The glass capillary array approaches to
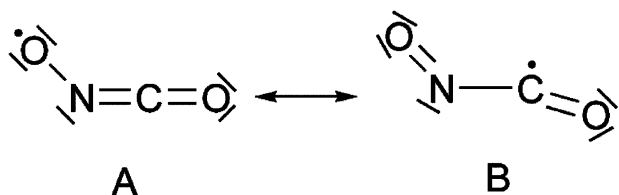
Fig. 1 The two resonance forms of the OCNO radical.

within 5 mm of the mirror during the condensation. The gases were condensed for 4 min at a pressure of 1.0×10^{-7} Torr at 10 K to a total thickness of 150 ± 50 nm. The ice sample was then irradiated isothermally with 5 keV electrons to cleave the nitrogen–nitrogen triple bond. The electron beam was operated at a nominal current of 100 nA with an extraction efficiency of 78.8% and scanned over the sample area 3.0 ± 0.4 cm^2 to avoid heating the ice. The sample was irradiated for 1 h, which exposed the target to 1.8×10^{15} electrons; longer irradiation times and higher beam currents should be avoided to eliminate overlapping electron trajectories and heating the ice surface.[6] In this work, four experiments were performed using (a) a molecular nitrogen ($^{14}N_2$) : carbon dioxide (CO_2) ice mixture (1 : 1), (b) a $^{15}N_2$: CO_2 ice mixture (1 : 1), (c) a $^{14}N_2$: $^{15}N_2$: CO_2 ice mixture (0.5 : 0.5 : 1), and (d) a $^{14}N_2$: $^{13}CO_2$ ice mixture (1 : 1). The gas mixtures were maintained at a ratio of 3 : 1 (N_2 : CO_2) to account for fractionated condensation thus providing a 1 : 1 ratio in the ice sample. The progress of the reaction was monitored using a Nicolet 510 DX Fourier transform infrared spectrometer (FTIR). The spectrometer has a wavelength range of 6000–500 cm^{-1} and operates in absorption–reflection–absorption mode with a reflection angle of 75° from the normal relative to the mirror surface. The infrared spectra of the ice were recorded online and *in situ* at an integrated time of 2.5 min and at a resolution of 2 cm^{-1}. The column densities of a molecule can be calculated according to Bennett *et al.*[6] Also, a quadrupole mass spectrometer is attached directly to the reaction chamber and can detect molecules that have sublimed into the gas phase.

3. Results

The experiment was carried out in three phases. First, the nitrogen : carbon dioxide ices were irradiated for a 1 h period of time. From this we can discuss the band assignments for the OCNO radical(s) as well as the kinetics of reaction. Second, the electron source was turned off and the sample was left for 1 h in the isothermal phase to check the stability of the radical(s) at 10 K. In the final phase of the experiment, the sample was warmed at a rate of 0.5 K min^{-1} to see when the OCNO infrared band begins to decrease in intensity indicating reaction of the nitroformyl radical, dissociation, and/or sublimation into the gas phase.

3.1 Infrared band assignment

First, we will investigate the observed bands in the infrared spectrum after the 1 h irradiation of the nitrogen–carbon dioxide ice mixture and discuss the assignment for the OCNO radical (Fig. 2). For comparison we have carried out *ab initio* vibrational frequency calculations for several isotopomers of the nitroformyl radical at the QCISD/6-31G* level of theory (see Appendix). In the $^{14}N_2$: CO_2 ice mixture, OC^{14}NO (X $^2A''$) was identified by its most intense vibration (ν_1, C=O stretch) which was found to be centered at 2113 cm^{-1} (Table 1). In comparison with our calculated frequency of 2138 cm^{-1}, there is good agreement after scaling of the theoretical value by 0.99. The next most intense absorption for the nitroformyl radical is the ν_3 (NC stretch) calculated to be at 964 cm^{-1}. However, this band is predicted to be 18 times less intense than the ν_1 vibration and would therefore be comparable to the noise level in the experiment. This means isotopic substitutions must be used to further confirm the assignment of the OCNO radical. Next, a $^{15}N_2$: CO_2 irradiation experiment was carried out to produce the OC^{15}NO isotopically labeled molecule. Upon analysis of the infrared spectrum after irradiation, the peak position remained unchanged at 2113 cm^{-1}. The theoretical calculations predict a slight redshift of 2 cm^{-1} from the ^{14}N isotope; this is within the limit of the resolution of the
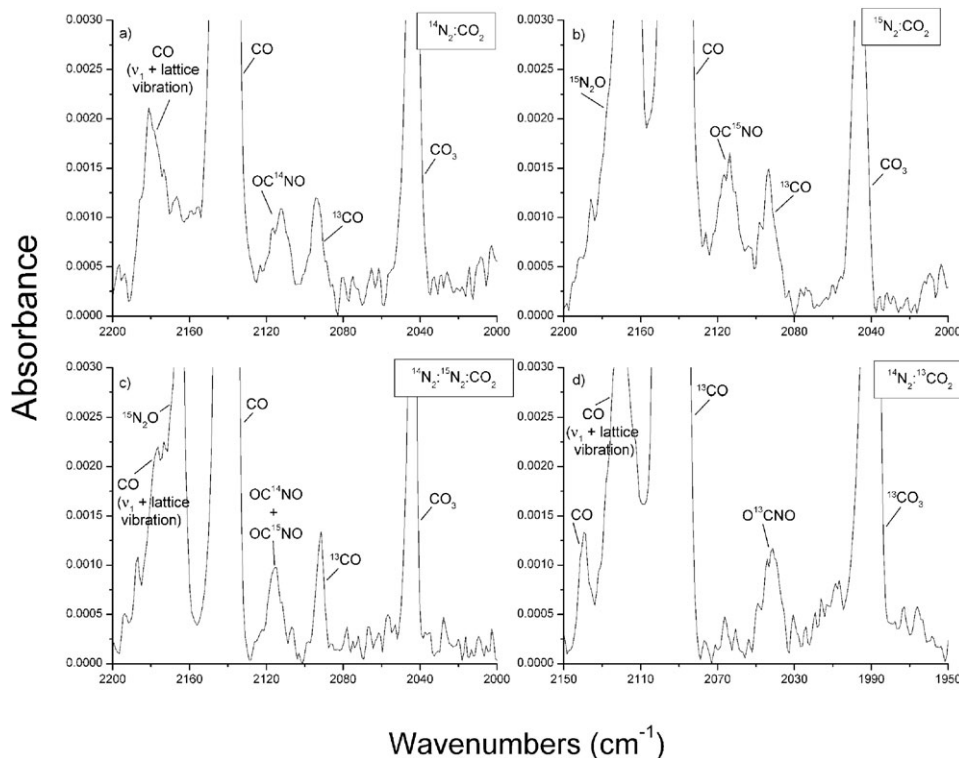

Fig. 2 The infrared bands for the ν_1 vibration of the OCNO radical are shown for the four isotopomers (initial reactants are boxed). Other observed absorptions include the ν_1 vibrations of carbon monoxide, carbon trioxide, and nitrous oxide.

Table 1 The observed frequencies of the ν_1 vibration of different isotopomers of the OCNO radical are compared with unscaled theoretically calculated frequencies at the QCISD/6-31G* level of theory

Isotopomer	Experimental frequency/cm^{-1}	Calculated frequency/cm^{-1}
OC^{14}NO	2113	2138
OC^{15}NO	2113	2136
OC^{14}NO + OC^{15}NO	2116	—
O^{13}CNO	2042	2080

Table 2 Rate constants were derived for the formation of the OCNO radical assuming pseudo-first order kinetics as discussed in the text

Isotopomer	k/s^{-1}	a/molecules cm^{-2}
OC^{14}NO (2113 cm^{-1})	$10.0 \pm 0.8 \times 10^{-4}$	$6.4 \pm 0.2 \times 10^{13}$
OC^{15}NO (2113 cm^{-1})	$9.3 \pm 2.0 \times 10^{-4}$	$1.3 \pm 0.1 \times 10^{14}$
OC^{14}NO + OC^{15}NO (2116 cm^{-1})	$9.5 \pm 0.5 \times 10^{-4}$	$9.7 \pm 0.2 \times 10^{13}$

spectrometer. Also, other factors can affect the peak position such as ice composition, sample thickness, sample temperature, impurities, or condensation rate which can influence the crystal structure and therefore the environment in which the OCNO radical would be vibrationally excited. Even though these variables are well constrained in our experiments, the small shift may not be observable as the nitrogen mass has little effect on the ν_1, C=O stretching frequency. In fact, this 2113 cm^{-1} band must result from irradiation of the N$_2$: CO$_2$ mixture since the band was not observed in similar irradiation experiments of pure nitrogen or carbon dioxide ices.[6,7] A third experiment was carried out by irradiating a ^{14}N$_2$: ^{15}N$_2$: CO$_2$ ice mixture. This would generate both isotopomers (OC^{14}NO and OC^{15}NO) so that we could hopefully be able to resolve two bands near 2113 cm^{-1}. Instead, only one band was observed at 2116 cm^{-1} indicating that the two isotopomers had irresolvable overlapping bands. This agrees with the similar band positions found for OC^{14}NO and OC^{15}NO in the two previous experiments. Lastly, in an irradiated ice mixture of ^{14}N$_2$: ^{13}CO$_2$, the nitroformyl radical (O^{13}CNO) was observed at 2042 cm^{-1} compared to the theoretical value of 2080 cm^{-1}; after scaling by 0.98, both the computed and experimental values agree very well. The ν_1, O^{13}CNO band (2042 cm^{-1}) is of similar intensity to the ν_1 vibrations of OC^{14}NO (2113 cm^{-1}) and OC^{15}NO (2113 cm^{-1}) mentioned earlier (Fig. 2) and the frequency shifts are in excellent agreement with the calculations. This supports the argument that the same molecule is responsible for the 2042 cm^{-1} band of the ^{14}N$_2$: ^{13}CO$_2$ experiment and the 2113 cm^{-1} bands from the ^{14}N$_2$: CO$_2$ and ^{15}N$_2$: CO$_2$ irradiation experiments; in comparison with the calculated frequencies, it also supports the assignment of the nitroformyl radical. As discussed in the following section, the kinetics analysis strengthens our identification of the OCNO radical (C_s, X ^{2}A″).

4. Discussion

4.1 Kinetics and dynamics

The lack of any previous detection of the nitroformyl radical indicates to either its difficulty of formation, ease of destruction or both. With this first experimental identification of the molecule in the present work, it is left to be explained why it has remained so elusive to the experimenter. To answer this we will first investigate the kinetics of its formation and then discuss possible reaction pathways to form the nitroformyl radical. The infrared vibration bands for the OCNO isotopomers (OC^{14}NO, 2113 cm^{-1}; OC^{15}NO, 2113 cm^{-1}; and OC^{14}NO + OC^{15}NO, 2116 cm^{-1}) were integrated during the irradiation to derive column densities for the molecule; please refer to ref. 6 for the detailed procedure. These column densities were plotted *versus* the irradiation time to provide the temporal evolution of the column densities of the nitroformyl radical. The temporal evolution of the column density of the nitroformyl radical looks to follow pseudo-first order kinetics for all isotopomers. The plots were therefore fit according to eqn (2). Here, a is the pre-exponential factor and k is the rate constant for the formation of the nitroformyl radical. Rate constants were derived for the OCNO peak

evolution of the three aforementioned experiments and the results are consistent with each other, shown in Table 2. Differences in the pre-exponential factor (a) can be accounted for by a number of factors including varying ice thicknesses or molecular ratios in the ice between experiments or because of the kinetic isotope effect. After weighing these factors, the kinetic parameters from the three experiments seem to be in agreement. The plot of the temporal evolution of the column density of the 2116 cm^{-1} peak resulting from irradiation of the ^{14}N$_2$: ^{15}N$_2$: CO$_2$ ice mixture is shown in Fig. 3 where the rate constant was fit to be $9.5 \pm 0.5 \times 10^{-4}$ s^{-1}. This peak was chosen because the fitting parameters (k and a) are closest to the average of the three fits.

$$[OCNO](t) = a \times (1 - e^{-kt}) \qquad (2)$$

We can now begin to discuss the formation route of the nitroformyl radical. Since the column density of the OCNO radical plotted over time fits a pseudo-first order equation, this precludes formation pathways between higher-order reactants. We can therefore eliminate pathways like CO + NO, O + CNO (NCO), C + NO$_2$, and O$_2$ + CN that would require at least two reaction steps to form the reactants. Instead, a more likely pathway to form OCNO in our experiment, which can explain the observed kinetics, is the electron induced decomposition of the nitrogen molecule in the carbon dioxide–nitrogen complex followed by the formation of OCNO *via* reaction of the generated nitrogen atoms with carbon dioxide, eqn (3).

$$N(^4S/^2D) + CO_2(X\ ^1\Sigma_g^+) \xrightarrow{k} OCNO(X\ ^2A'') \qquad (3)$$
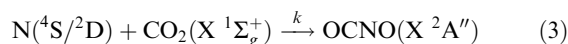
Fitting the column density of the nitroformyl radical with pseudo-first order kinetics as we have done with eqn (2), and assuming the primary formation pathway to OCNO is shown in eqn (3), this means that the time it takes to dissociate a nitrogen molecule producing two nitrogen atoms is negligible
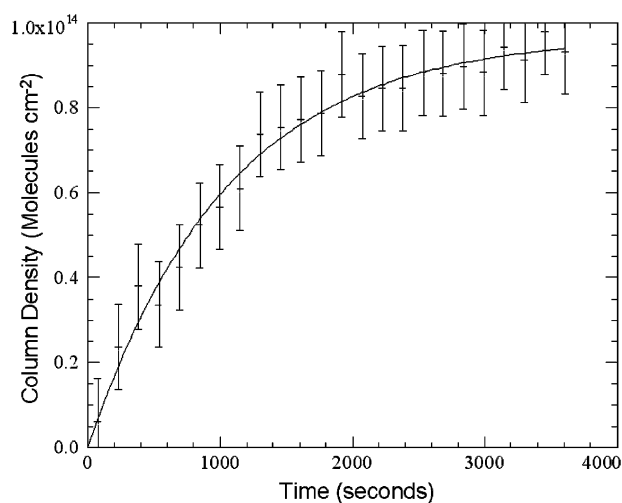
Fig. 3 The temporal development of the column density of the OCNO radical during the 1 h irradiation phase of the ^{14}N$_2$: ^{15}N$_2$: CO$_2$ experiment is shown with a best fit from eqn (2). Error bars are $\pm 10^{13}$ molecules cm^{-2}; calculated by integrating a featureless region of the infrared spectra and propagating this error through the column density calculations.
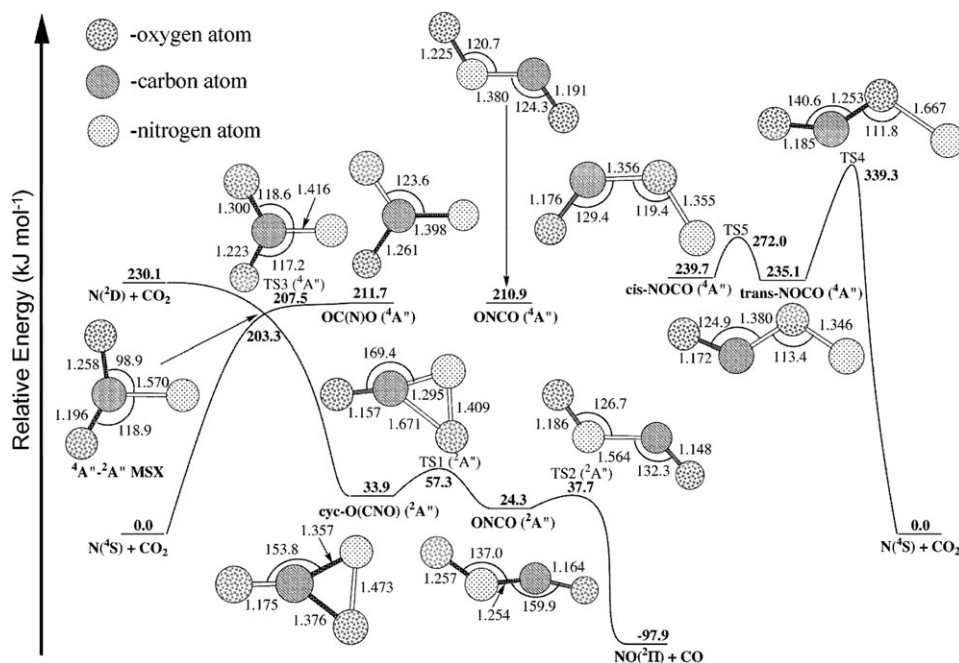
Fig. 4 The potential energy surface (PES) for the N + CO$_2$ reaction. Relative energies are in units of kJ mol^{-1}. The relative energy of OCNO(^{2}A″) with respect to N(^{4}S) + CO$_2$ is shown as evaluated at the coupled cluster CCSD(T) level[15] at the complete basis set (CBS) limit. It is obtained from the energies calculated at CCSD(T) with Dunning's correlation-consistent cc-pVDZ, cc-pVTZ, cc-pVQZ, and cc-pV5Z basis sets extrapolated to the CBS limit. For the other intermediates and transition states, relative energies are computed at the CCSD(T)/6-311+G(3df) level with respect to OCNO(^{2}A″) and then shifted by the energy difference between OCNO(^{2}A″) and N(^{4}S) + CO$_2$ obtained at CCSD(T)/CBS. All energies include zero-point energy (ZPE) corrections computed at the density functional B3LYP/6-311G** level of theory. The energy of N(^{2}D) + CO$_2$ relative N(^{4}S) + CO$_2$ is taken from experimental reference data,[16] because the single-reference CCSD(T)/6-311+G(3df) method is not able to describe the quartet-doublet energy gap of the N atom accurately and overestimates its value by 33 kJ mol^{-1}. Geometric parameters are optimized at B3LYP/6-311G**. The minimum on the seam of crossing (MSX) between the ^{4}A″ and ^{2}A″ PESs is optimized at the CASSCF/6-311G** level with the (17,14) active space, which included all valence electrons and valence orbitals except 2s orbitals of oxygen atoms and then its relative energy is refined at CCSD(T)/6-311+G(3df). GAUSSIAN 98[17] and MOLPRO 2002[18] programs were used for all calculations.

with respect to the speed of reaction of the nitrogen atom shown in eqn (3). According to the column density profile in Fig. 3, this seems to be the case. Through electronic energy transfer processes, the nitrogen molecule can undergo homolytic bond cleavage by predissociation of a bound singlet state which has been electronically excited from the ground state. The two nitrogen atoms will be mostly produced in the excited electronic state (^{2}D) and in the ground electronic state (^{4}S), the exact ratio being largely dependent on the amount of energy absorbed by the nitrogen molecule.[8,9] These nitrogen atoms can then react with a carbon dioxide molecule as shown in eqn (3). In comparison, this reaction was also studied in the gas phase where the internally excited OCNO intermediate could not be stabilized *via* phonon coupling; the reaction complex was found to immediately dissociate to CO + NO.[10,11] The rate constant for this reaction was derived to be 3.2 × 10^{-13} cm^3 s^{-1}.[10]

How is this proposed mechanism supported by our electronic structure calculations? The energetics of the reaction (eqn (3)) are graphically represented in Fig. 4 in the NCO$_2$ potential energy surface (PES). Let us first discuss the energetics associated with the doublet surface. If nitrogen atoms are produced in their electronically excited state (^{2}D), they can react with a carbon dioxide molecule. The nitrogen attack can be directed to either one of the double bonds of the O=C=O molecule to form the cyclic O(CNO) molecule on the doublet surface. This reaction proceeds without barrier and is exoergic by 196.2 kJ mol^{-1}. This excess internal energy must be diverted to the surrounding matrix or the molecule will not be stabilized. Recall that in a previous experiment investigating the O + CO$_2$ reaction, Bennett *et al.*[6] observed the cyclic CO$_3$(C_{2v}, ^{1}A$_1$) isomer which was found to be stable. However, the cyclic O(CNO) molecule was not detected in the infrared spectra of our experiments indicating that this molecule may not be stabilized under our experimental conditions. However, in all

four experiments using different isotopically labeled species, the predicted vibrational frequencies for the most intense peak of the cyclic NCO$_2$ molecule directly overlaps with the intense ν_1 vibration from the CO$_3$ molecule, which was also produced during irradiation. This may therefore be the only reason that the cyclic O(CNO) molecule was undetected. Both molecules (cyclic NCO$_2$ and cyclic CO$_3$) have similar barriers to isomerization and similar reaction mechanisms and energies, so their stabilities must result from the efficiency at which they can divert the excess energy from formation. If the cyclic O(CNO) molecule was indeed found to be inefficient at releasing its internal energy, it would ring open to the observed bent OCNO radical. This isomerization process requires an energy barrier of 23.4 kJ mol^{-1} (transition state 1, TS1), energy that is readily available if the 196.2 kJ mol^{-1} from formation of the cyclic (OCNO) molecule are bound in internal modes. The bent OCNO radical exists 9.6 kJ mol^{-1} below the cyclic isomer but seems to sufficiently be able to dissipate its internal energy to the matrix and stabilize, evidenced by its detection. Otherwise, as indicated in eqn (1), the bent OCNO radical can dissociate along its central CN bond to yield carbon monoxide and nitric oxide. The barrier to dissociation is calculated to be 13.4 kJ mol^{-1} (TS2) with a total exoergicity of 122.2 kJ mol^{-1}. These values are in agreement with those reported in the Introduction section.

On the quartet surface there exists a large barrier for a nitrogen atom (^{4}S) to react with a carbon dioxide molecule. However, if a nitrogen molecule dissociates into two ground state nitrogen atoms, these atoms are likely to carry excess kinetic energy (suprathermal), which would allow them to overcome this reaction entrance barrier. As seen in the PES (Fig. 4), there exists a conical intersection 203.3 kJ mol^{-1} above the separated reactants on the quartet surface. Here, a reacting suprathermal nitrogen atom in the ground state and a carbon dioxide molecule can switch from the quartet surface to

the doublet surface and then proceed to react as previously discussed. It is unknown which is the predominant spin state for dissociated nitrogen atoms, so it is therefore difficult to comment on the original entrance channel (quartet *versus* doublet). The potential energy surface also indicates various reactions where the nitrogen atom will bond to an oxygen atom of the carbon dioxide molecule. However, it is unclear that there is an energetically accessible isomerization pathway to reach the observed OCNO radical and, therefore, there will be no discussion about this part of the PES.

4.2 OCNO stability

As discussed in the previous section, the OCNO radical is very efficient at diverting its internal energy to the matrix material thereby thermalizing and becoming stable at 10 K. This is reflected in the isothermal phase of the experiment. After irradiation was stopped, the sample was kept at 10 K to check the stability of the OCNO radical. There was no decrease in its infrared band intensity indicating that the nitroformyl molecule has a long lifetime in this low temperature environment. The sample was then warmed at a rate of 0.5 K min^{-1}. Interestingly, the OCNO absorption feature did not begin to decrease until about 60 K and was detectable until about 100 K. Normally radicals are quickly destroyed through reactions with other molecules or atoms. However this assumes that they can react without barrier to products that are energetically lower than the reactants. In the current experiment, the reactants that are expected to exist with the most abundance in the ice after irradiation are N$_2$, CO$_2$, and CO as well as ground state nitrogen and oxygen atoms. The nitrogen molecule, carbon dioxide, and carbon monoxide are very stable closed-shell molecules that should not readily react with the OCNO radical. Also, the nitrogen and oxygen atoms reacting with OCNO would most likely form high energy products discounting the possibility for reaction in a thermally equilibrated low temperature ice. This could justify the stability of the OCNO radical until the higher temperatures. However, the disappearance of the OCNO radical is not fully resolved. In one scenario, the nitroformyl radical could undergo a reaction where the pathway only becomes allowed (due to diffusion of the species in the ice) or becomes energetically available above 60 K. But it is not apparent which reactions, if any, take place that contribute to the destruction of the OCNO radical. Another explanation could be due to sublimation into the gas phase. However, after analyzing the quadrupole mass spectrometer signal, there was no evidence of OCNO or its predicted fragment species (CO + NO, simultaneously) in the gas phase. A final explanation that could contribute to the disappearance of the OCNO radical is by a dissociation of the central CN bond in eqn (1). At 60 K, the temperature at which the infrared band of the nitroformyl radical was observed to decrease, the rate constant k for OCNO dissociation was calculated from eqn (4). Here, k_B is the Boltzman constant, $\Delta_R G$ is the free-energy change from OCNO to the transition state (13.25 kJ mol^{-1}), R is the universal gas constant, and T is the temperature.

$$k = (k_B T/h) \exp(-\Delta_R G/RT) \qquad (4)$$

Using transition state theory in conjunction with Gibbs energies for OCNO and the dissociation transition state obtained from our *ab initio* calculations, one obtains the following dissociation rate constants for the temperature range 60–100 K: $k(60\ K) = 3.90 \times 10^0$ s^{-1}; $k(70\ K) = 2.13 \times 10^2$ s^{-1}; $k(80\ K) = 4.39 \times 10^3$ s^{-1}; $k(90\ K) = 4.70 \times 10^4$ s^{-1}; $k(100\ K) = 3.17 \times 10^5$ s^{-1}. A fit to the Arrhenius equation of the calculated rate constants for the temperature range 5–100 K gave the following result (eqn (5)).

$$k = 2.21 \times 10^{12} \exp(-13.519\ kJ/RT) \qquad (5)$$

Thus, the dissociation rate is quite substantial at 60 K, and this dissociation reaction should play a major role in the disappearance of the nitroformyl radical as the temperature increases.

5. Conclusion

The nitroformyl radical was detected *via* its ν_1 vibration centered at 2113 cm^{-1} for both the OC^{14}NO and OC^{15}NO isotopomers. The O^{13}CNO molecule was observed at 2042 cm^{-1}. These C=O stretching frequencies agree with our theoretically predicted data presented in Table 1. The kinetics also support the OCNO assignment since pseudo-first order kinetics would be expected assuming the nitroformyl radical is formed by the N + CO$_2$ reaction from eqn (3). This pathway would require a minimum excess energy of 203.3 kJ mol^{-1} (2.1 eV) from the nitrogen atom reactants; either in electronic energy or kinetic energy. This outlines the importance of non-equilibrium chemistry, where the reactants are not thermalized with the 10 K ice. The reaction then proceeds through a cyclic intermediate O(CNO) that may not be stabilized in the matrix, but rather a ring opens along the C–O bond to yield the bent OCNO radical as outlined in the potential energy surface (Fig. 4). The OCNO radical then diverts its internal energy to nearby matrix molecules and relaxes into a stable state.

This process has relevance to such environments as in the icy mantles on dust grains in the interstellar medium, or on the icy surface of Triton, Neptune's largest moon, where nitrogen and carbon dioxide are likely to be chemically processed by the harsh radiation environment that exists in space.[12] The keV electrons used in this experiment actually simulate the radiation effects of a typical galactic cosmic ray proton as it penetrates an ice surface.[13] Therefore, when searching for a natural environment where the OCNO radical might exist, low temperature ices in astrophysical regions are likely candidates. Also, a detection of the OCNO radical in interstellar space could be used to derive the abundance of the infrared inactive nitrogen molecule. This has previously been suggested using the azide radical (N$_3$, X $^2\Pi_g$).[14] However, the absorption coefficient of the OCNO radical is twice as large[12] and may prove more useful for quantifying the molecular nitrogen abundance in carbon dioxide rich ices.

Appendix

Vibrational frequency calculations were performed for several molecules and isotopomers that are relevant to the N + CO$_2$ reaction potential energy surface (Fig. 4). The computations were carried out at the QCISD/6-31G* level of theory.

Molecule/ Isotopomer	Vibrational mode	Vibrational frequency/ cm^{-1}	Intensity/ cm molecule^{-1}
bent OCNO (^{2}A″)			
^{16}O^{12}C^{14}N ^{16}O	a′	212.8	2.71×10^{-18}
	a″	336.2	3.32×10^{-18}
	a′	612.6	4.00×10^{-18}
	a′	964.2	4.62×10^{-18}
	a′	1327.3	3.47×10^{-18}
	a′	2138.0	8.54×10^{-17}
^{16}O^{13}C^{14}N ^{16}O	a′	211.0	2.64×10^{-18}
	a″	326.4	3.11×10^{-18}
	a′	600.1	3.97×10^{-18}
	a′	959.4	4.72×10^{-18}
	a′	1327.1	3.46×10^{-18}
	a′	2080.9	8.05×10^{-17}
^{16}O^{12}C^{15}N ^{16}O	a′	211.0	2.67×10^{-18}
	a″	336.0	3.32×10^{-18}
	a′	609.0	3.95×10^{-18}

(*continued*)

Molecule/ Isotopomer	Vibrational mode	Vibrational frequency/ cm^{-1}	Intensity/ cm molecule^{-1}
	a′	955.0	4.25×10^{-18}
	a′	1298.0	3.36×10^{-18}
	a′	2136.0	8.51×10^{-17}
$^{18}O^{12}C^{14}N\ ^{18}O$	a′	207.0	2.56×10^{-18}
	a″	332.0	3.29×10^{-18}
	a′	602.0	3.65×10^{-18}
	a′	932.0	4.68×10^{-18}
	a′	1301.0	3.36×10^{-18}
	a′	2104.0	8.35×10^{-17}
$^{18}O^{12}C^{15}N\ ^{18}O$	a′	205.0	2.52×10^{-18}
	a″	331.0	3.27×10^{-18}
	a′	599.0	3.62×10^{-18}
	a′	922.0	4.29×10^{-18}
	a′	1272.0	3.22×10^{-18}
	a′	2102.0	8.32×10^{-17}
$^{16}O^{13}C^{15}N\ ^{16}O$	a′	209.0	2.61×10^{-18}
	a″	326.3	3.10×10^{-18}
	a′	595.7	3.92×10^{-18}
	a′	949.8	4.34×10^{-18}
	a′	1298.1	3.32×10^{-18}
	a′	2079.0	8.02×10^{-17}
$^{18}O^{13}C^{14}N\ ^{18}O$	a′	204.8	2.49×10^{-18}
	a″	321.7	3.08×10^{-18}
	a′	589.8	3.63×10^{-18}
	a′	927.7	4.73×10^{-18}
	a′	1301.2	3.32×10^{-18}
	a′	2045.6	7.86×10^{-17}
$^{18}O^{13}C^{15}N\ ^{18}O$	a′	202.8	2.46×10^{-18}
	a″	321.5	3.06×10^{-18}
	a′	586.0	3.60×10^{-18}
	a′	917.8	4.34×10^{-18}
	a′	1271.7	3.19×10^{-18}
	a′	2043.3	7.83×10^{-17}
cyc-O(CNO) (^{2}A″)			
$^{16}O^{12}C^{14}N\ ^{16}O$	a′	556.2	1.75×10^{-18}
	a″	594.5	5.80×10^{-18}
	a′	639.4	2.43×10^{-18}
	a′	965.2	8.62×10^{-18}
	a′	1084.6	2.52×10^{-18}
	a′	2073.5	6.50×10^{-17}
$^{16}O^{13}C^{14}N\ ^{16}O$	a′	552.3	1.73×10^{-18}
	a″	576.5	5.45×10^{-18}
	a′	636.6	2.55×10^{-18}
	a′	944.2	8.11×10^{-18}
	a′	1082.7	2.46×10^{-18}
	a′	2017.3	6.09×10^{-17}
$^{16}O^{13}C^{15}N\ ^{16}O$	a′	546.9	1.63×10^{-18}
	a″	575.3	5.45×10^{-18}
	a′	627.7	2.52×10^{-18}
	a′	938.7	7.70×10^{-18}
	a′	1069.8	2.98×10^{-18}
	a′	2015.7	6.09×10^{-17}
$^{16}O^{12}C^{15}N\ ^{16}O$	a′	551.0	1.64×10^{-18}
	a″	593.0	5.78×10^{-18}
	a′	630.0	2.41×10^{-18}
	a′	960.0	8.11×10^{-18}
	a′	1072.0	3.12×10^{-18}
	a′	2072.0	6.49×10^{-17}
$^{18}O^{12}C^{14}N\ ^{18}O$	a′	538.0	1.76×10^{-18}
	a″	589.0	5.65×10^{-18}
	a′	622.0	2.04×10^{-18}
	a′	949.0	9.19×10^{-18}
	a′	1048.0	1.43×10^{-18}
	a′	2041.0	6.36×10^{-17}

(*continued*)

Molecule/ Isotopomer	Vibrational mode	Vibrational frequency/ cm^{-1}	Intensity/ cm molecule^{-1}
$^{18}O^{12}C^{15}N\ ^{18}O$	a′	533.0	1.66×10^{-18}
	a″	588.0	5.65×10^{-18}
	a′	613.0	2.19×10^{-18}
	a′	945.0	8.69×10^{-18}
	a′	1034.0	1.98×10^{-18}
	a′	2039.0	6.35×10^{-17}
$^{18}O^{13}C^{14}N\ ^{18}O$	a′	534.8	1.74×10^{-18}
	a″	570.7	5.32×10^{-18}
	a′	619.4	2.15×10^{-18}
	a′	927.5	8.57×10^{-18}
	a′	1047.1	1.46×10^{-18}
	a′	1983.5	5.96×10^{-17}
$^{18}O^{13}C^{15}N\ ^{18}O$	a′	529.7	1.64×10^{-18}
	a″	569.5	5.31×10^{-18}
	a′	610.3	2.13×10^{-18}
	a′	923.1	8.20×10^{-18}
	a′	1032.6	1.91×10^{-18}
	a′	1981.7	5.95×10^{-17}
branch OC(N)O (^{4}A″)	a′	376.2	5.17×10^{-18}
	a′	584.9	2.68×10^{-18}
	a′	587.9	9.96×10^{-18}
	a′	936.1	1.76×10^{-19}
	a′	1111.5	9.74×10^{-18}
	a′	1445.6	9.10×10^{-18}
chain OCNO (^{4}A″)	a″	255.9	5.18×10^{-19}
	a′	298.1	8.62×10^{-19}
	a′	608.3	2.25×10^{-19}
	a′	1042.1	1.15×10^{-17}
	a′	1591.1	1.18×10^{-18}
	a′	1808.4	2.55×10^{-17}
cis-NOCO (^{4}A″)	a′	250.8	2.29×10^{-19}
	a″	392.9	5.21×10^{-19}
	a′	757.2	2.37×10^{-18}
	a′	938.2	5.33×10^{-18}
	a′	998.9	3.84×10^{-17}
	a′	1892.9	4.66×10^{-17}
trans-NOCO (^{4}A″)	a″	224.7	6.23×10^{-19}
	a′	362.8	8.11×10^{-19}
	a′	600.4	6.68×10^{-20}
	a′	967.0	3.08×10^{-17}
	a′	1112.7	3.03×10^{-17}
	a′	1921.8	4.33×10^{-17}

References

1 B. D. Benson and J. S. Francisco, *Chem. Phys. Lett.*, 1995, **233**, 335.

2 J. J. Liu, Y. H. Ding, Y. G. Tao, J. K. Feng and C. C. Sun, *J. Comput. Chem.*, 2002, **23**, 1031.

3 J. X. Zhang, J. Y. Liu, Z. S. Li and C. C. Sun, *J. Comput. Chem.*, 2004, **25**, 1888.

4 A. A. Korkin, A. Lowrey, J. Leszczynski, D. B. Lempert and R. J. Bartlett, *J. Phys. Chem. A*, 1997, **101**, 2709.

5 A. L. Cooksy, *J. Am. Chem. Soc.*, 2001, **123**, 4003.

6 C. J. Bennett, C. Jamieson, A. M. Mebel and R. I. Kaiser, *Phys. Chem. Chem. Phys.*, 2004, **6**, 735.

7 C. S. Jamieson, A. M. Mebel and R. I. Kaiser, in preparation.

8 V. I. Shematovich, D. V. Bisikalo and J. C. Gerard, *Ann. Geophys.*, 1992, **10**(10), 792.

9 C. W. Walter, P. C. Cosby and H. Helm, *J. Chem. Phys.*, 1993, **99**(5), 3553.

10 L. I. Avramenko and V. M. Kransnen'kov, *Bull. Acad. Sci. USSR Div. Chem. Sci. (Engl. Transl.)*, 1967, 501.

11 J. T. Herron and R. E. Huie, *J. Phys. Chem.*, 1968, **72**, 2235.

12 C. S. Jamieson, C. J. Bennett, A. M. Mebel and R. I. Kaiser, *Astrophys. J.*, 2005, **624**, 436.

13 C. S. Jamieson, A. M. Mebel and R. I. Kaiser, *Astrophys. J.*, 2005, in press.

14 R. L. Hudson and M. H. Moore, *Astrophys. J.*, 2002, **568**, 1095.

15 For the description of various quantum chemical methods and basis sets, see C. J. Cramer, *Essentials of Computational Chemistry. Theories and Models*, Wiley, New York, 2002.

16 NIST Atomic Spectra Data Base, Version 3.0, February 2005, http://physics.nist.gov/cgi-bin/AtData/main_asd.

17 M. J. Frisch, G. W. Trucks, H. B. Schlegel, G. E. Scuseria, M. A. Robb, J. R. Cheeseman, V. G. Zakrzewski, J. A. Montgomery, R. E. Stratmann, J. C. Burant, S. Dapprich, J. M. Millam, R. E. Daniels, K. N. Kudin, M. C. Strain, O. Farkas, J. Tomasi, V. Barone, M. Cossi, R. Cammi, B. Mennucci, C. Pomelli, C. Adamo, S. Clifford, J. Ochterski, G. A. Petersson, P. Y. Ayala, Q. Cui, K. Morokuma, P. Salvador, J. J. Dannenberg, D. K. Malick, A. D. Rabuck, K. Raghavachari, J. B. Foresman, J. Cioslowski, J. V. Ortiz, A. G. Baboul, B. B. Stefanov, G. Liu, A. Liashenko, P. Piskorz, I. Komaromi, R. Gomperts, R. L. Martin, D. J. Fox, T. Keith, M. A. Al-Laham, C. Y. Peng, A. Nanayakkara, M. Challacombe, P. M. W. Gill, B. Johnson, W. Chen, M. W. Wong, J. L. Andres, C. Gonzalez, M. Head-Gordon, E. S. Replogle, J. A. Pople, *GAUSSIAN 98 (Revision A.11)*, Gaussian, Inc., Pittsburgh, PA, 2001.

18 *MOLPRO* is a package of *ab initio* programs written by, H.-J. Werner, P. J. Knowles, M. Schütz, R. Lindh, P. Celani, T. Korona, G. Rauhut, F. R. Manby, R. D. Amos, A. Bernhardsson, A. Berning, D. L. Cooper, M. J. O. Deegan, A. J. Dobbyn, F. Eckert, C. Hampel, G. Hetzer, A. W. Lloyd, S. J. McNicholas, W. Meyer, M. E. Mura, A. Nicklaß, P. Palmieri, R. Pitzer, U. Schumann, H. Stoll, A. J. Stone, R. Tarroni and T. Thorsteinsson, University College Cardiff Consultants Ltd., 2004.